

# Three-Dimensional Finite Element Analysis of Tieback Walls in Sand

Lim, Yu-Jin\*<sup>1</sup>

Briaud, Jean-Louis\*<sup>2</sup>

---

---

## 요 지

비선형 3차원 유한요소 해석법을 이용하여 타이백으로 억지된 토류벽의 거동을 분석하여 설계 시에 고려되는 중요 파라미터의 영향을 조사하였다. 제안된 유한요소기법에서 엄지말뚝과 텐던 고정길이는 빔요소로, 토류판은 셸요소로, 텐던 비정착길이는 스프링 요소로 모델링 하였다.

사용된 흙의 거동모델은 사질토의 비선형 거동 특성과 응력이력을 고려할 수 있는 기존의 Hyperbolic 모델을 수정하여 사용하였으며 벽체 전면에서의 굴착, 타이백 설치, 타이조임 그리고 재굴착 등의 모든 축조과정을 단계별로 해석할 수 있는 시뮬레이션 기법을 제안하였다. 여러 가지 주요 설계인자를 변화시키며 파라메트릭 해석을 수행하였고 이 결과 앵커의 위치, 앵커의 비정착 길이, 앵커 조임하중의 크기 와 엄지말뚝의 근입깊이등의 영향을 밝혀낼 수 있었다. 이 해석 결과를 토대로 새로운 설계지침을 제안하였다.

## Abstract

A three dimensional nonlinear finite element analysis is used to study the influence of various design decisions for tieback walls. The numerical model simulates the soldier piles and the tendon bonded length of the anchors with beam elements, the unbonded tendon with a spring element, the wood lagging with the shell elements, and the soil with solid 3D nonlinear elements. The soil model used is a modified hyperbolic model with unloading hysteresis. The complete sequence of construction is simulated including the excavation, and the placement and stressing of the anchors. The numerical model is calibrated against a full scale instrumented tieback wall at the National Geotechnical Experimentation Site (NGES) on the Riverside Campus of Texas A&M University. Then a parametric study is conducted.

The results give information on the influence of the following factors on the wall behavior: location of the first anchor, length of the tendon unbonded zone, magnitude of the anchor forces, embedment of the soldier piles, stiffness of the wood lagging, and of the piles. The implications in design are discussed.

---

\*<sup>1</sup> Member, Chief Researcher, Geotechnical Division, Highway Research Center, Korea Highway Corporation

\*<sup>2</sup> Spencer J. Buchanan Professor, Department of Civil Engineering, Texas A&M University

Keywords : Tieback Walls, Sand, Anchors, Pressure Distribution, Deflections, Finite Element Method, Nonlinear Soil Model, Three Dimensional Simulation, National Geotechnical Experimentation Site, Soldier Pile, Wood Lagging

---

## 1. Introduction

Most commonly, tieback walls (Fig. 1) are designed on the basis of a simple pressure diagram (Terzaghi and Peck, 1967) used to calculate the anchor loads and the bending moment profile in the piles. There is a growing trend in practice to design tieback walls by using the beam-column approach (Kim and Briaud, 1993; Halliburton, 1968; Matlock et al. 1981). This computer based solution is used to predict the bending moment, the axial load and the deflection profiles of the piles after the anchor loads have been chosen. Compared to the simple pressure diagram approach, the beam column approach leads to deflection predictions and to improved bending moment profiles; however, the predicted deflections are not as reliable as the bending moments because the model ignores the mass movement of the soil. The Finite Element Method (FEM) represents another level of sophistication which comes very close to modeling all the components involved (Clough, 1984). The drawback is that the FEM approach is very time consuming; therefore, it is generally performed at the research level or for very large projects.

A study on the use of the beam-column approach (Kim and Briaud, 1994) leads to detail

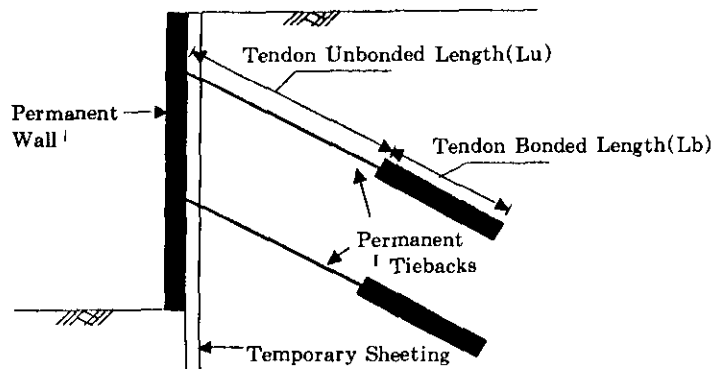


Fig.1 Schematic of a Tieback Wall

recommendations on how to best use that method. It also identified the inability of predicting reliable displacement profiles with this method because the model ignores mass movement. The FEM study described in this article was undertaken, after the beam-column study, to better simulate the deformation process and to evaluate the influ-

ence of various factors on the wall deflections. These factors include the location of the first anchor, the length of the tendon unbonded zone, the magnitude of the anchor forces, the embedment of the soldier piles, and the stiffness of the wood lagging and of the piles (Lim and Briaud, 1996).

## 2. Mesh Boundaries : How far is far Enough?

One of the first steps in any numerical simulation is to determine where to place the boundaries so that their influence on the results will be minimized. The boundary effect was studied while using a linear elastic soil. The bottom of the mesh is best placed at a depth where the soil becomes notably harder. If  $D$  is the distance from the bottom of the excavation to the hard layer, a value of  $D$  equal to 9m was used for nearly all analyses. This value of  $D$  came from the instrumented case history used to calibrate the FEM model because of the hard shale layer existing at that depth. It was shown (Lim and Briaud, 1996) that when using a elastic soil in the simulation,  $D$  has linear influence on the vertical movement of the ground surface at the top of the wall but comparatively very little influence on the horizontal movement of the wall face.

Considering the parameters  $H_c$ ,  $W_c$ ,  $B_c$ , and  $D$  as defined in Fig. 2, it was found in a separate study (Lim and Briaud, 1996) that  $W_c=3D$  and  $B_c=3(H_c+D)$  were appropriate values for  $W_c$  and  $B_c$ ; indeed beyond these values,  $W_c$  and  $B_c$  have little influence on the horizontal deflection of the wall due to the excavation of the soil. This confirms previous findings by Dunlop and Duncan (1970). For the instrumented wall to be simulated,  $H_c$  was 7.5m,  $D$  was 9m,  $B_c$  was 66m or  $4(H_c+D)$  and  $W_c$  was 10m. The small value of  $W_c$  was chosen because the U shape excavation for the case history was 20m wide.

## 3. Modeling of Tieback Wall

### 3.1 Simulated Wall Section

It would be possible to simulate the entire width of the wall in three dimensions. However, the size of the mesh would be prohibitively large. Instead, a repetitive section of the wall was chosen for the simulation. It was found that the best section (Fig. 3) would include one vertical pile at the center of the section, one stack of inclined anchors attached to the soldier pile and penetrating back into the soil, and the soil mass. The width of the mesh was equal to the pile spacing or 2.44m for the case history. Special movement restraints (Multi-Point Constraints: MPC) were developed on the vertical edge boundaries of the wall in order to maintain a right angle in plan view between the displaced wall face and the sides of the simulated wall section.

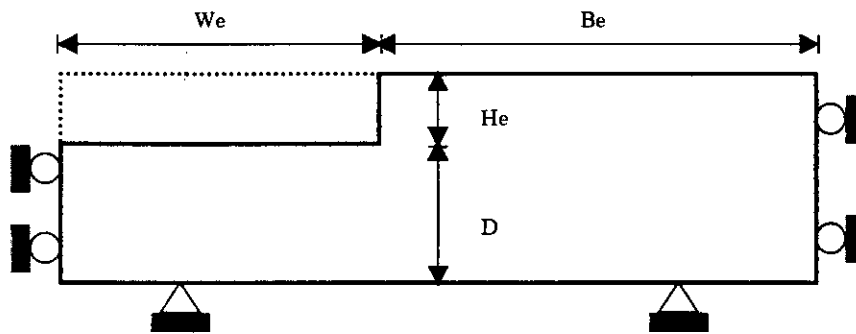


Fig.2 Definition of  $H_e$ ,  $W_e$ ,  $B_e$ , and  $D$

### 3.2 Modeling of Anchor Lock-off Loads

In the proposed method of simulation of the tieback wall, the tieback installation is simulated by applying a constant load at the location of the anchor head and the same constant load, but in opposite direction, at the top of the bonded zone of the tieback simultaneously as shown in Fig. 4. Then a spring is installed between these two loading points to simulate load changes in the tie rod. The load changes in the tie rod are generated due to difference in displacement changes between these two loading points which may be produced by subsequent construction activities such as excavation and prestressing of the

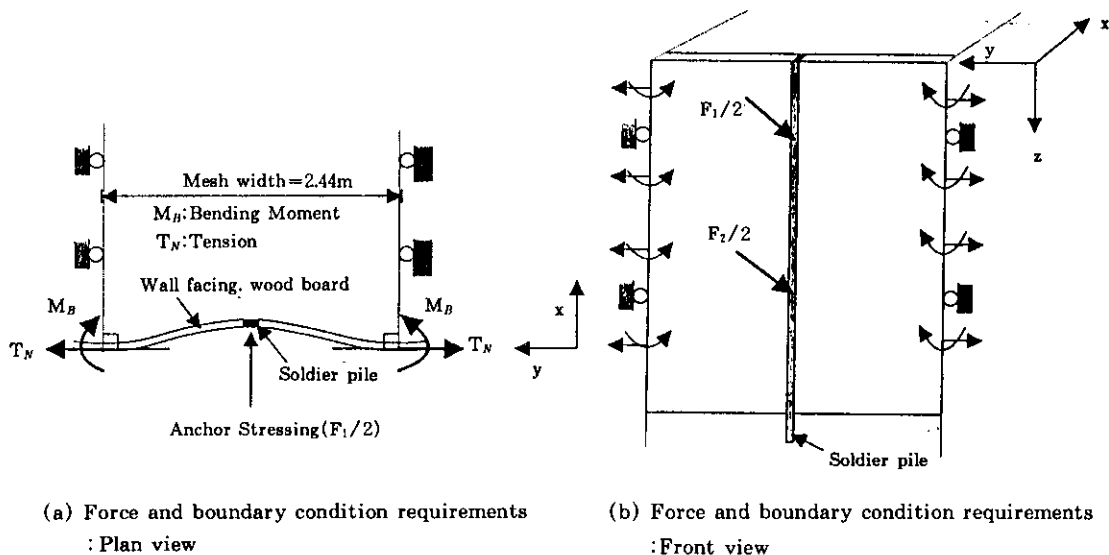


Fig.3 Simulated Repetitive Wall Section

lower anchors. The load changes in the tie rod are governed by the tendon stiffness. Therefore, anchor load variation can be observed with construction sequence. The spring behavior can be assumed to be linear or nonlinear, depending on the behavior of the tiebacks. If it is linear, a constant stiffness is provided. In the nonlinear case, the force is assumed to be a function of relative displacement in the spring. In this study, the behavior of the tieback was assumed to be linear so that a constant stiffness value was used throughout the analyses.

Since a soldier pile withstands one half of anchor lock-off load for each anchor as shown in Fig. 3 and Fig. 4, one half of tendon stiffness is used for the spring elements of the unbonded length to obtain the same wall deflection or anchor elongation.

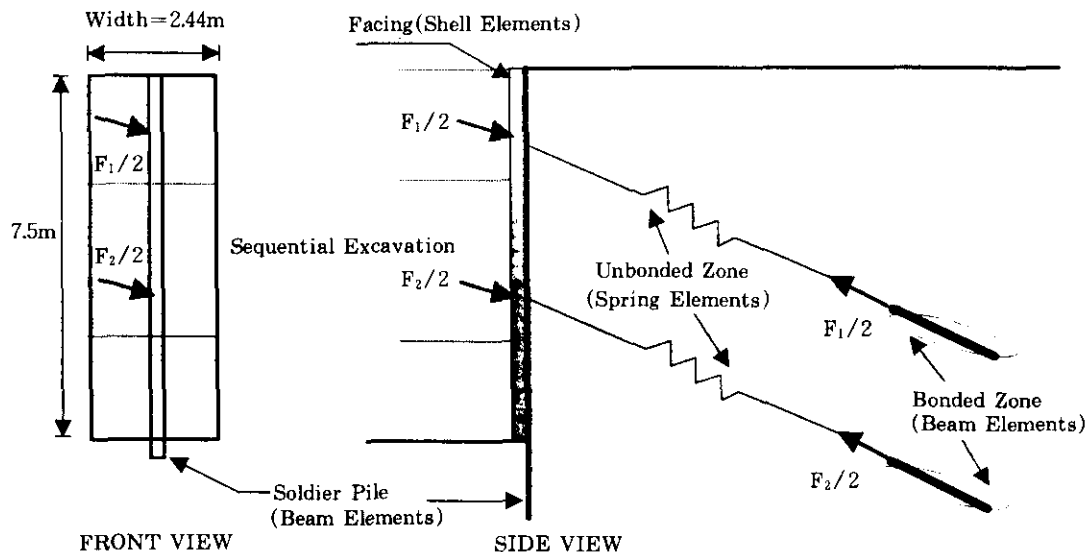


Fig.4 Schematics of Proposed Three Dimensional Finite Element Simulation

#### 4. Soil and Structure Element Models

The general purpose code ABAQUS(Hibbit, Karlson, Sorensen, Inc., 1992) was used for all the runs. The soldier piles and the tendon bonded length of the anchors were simulated with beam elements: these were 1D elements which can resist axial loads and bending moments. The stiffness for the pile elements was the EI and AE values of the soldier piles in the Texas A&M University tieback wall. The tendon bonded length was treated as a composite steel/grout section in order to get the EI and AE stiffness: a reduced grout modulus equal to 40% of the intact grout modulus was used to account for grout cracking. The wood lagging facing was simulated with shell elements: these are 2D elements which

can resist axial loads and bending moments in the two directions. The shell elements were given the thickness of the wooden boards and modulus of wood. The steel tendon in the tendon unbonded length of the anchor was simulated as a spring element, and this is an 1D element that can only resist axial load. This element was given a spring stiffness  $K$  equal to the initial slope of the load-displacement curve obtained in the anchor pull out tests (Chung and Briaud, 1993).

The soil was simulated with three dimensional 8 noded brick elements. The soil model was a modified Duncan-Chang hyperbolic model(Duncan et al., 1980). This model is a nonlinear model which includes the influence of the stress level on the stiffness, on the strength, and on the volume change characteristics of the soil. With this soil model it was also possible to simulate the hysteresis of the soil by unloading and reloading the soil along a path different from the loading path. The parameters necessary for the soil model included 7 parameters to describe the loading tangent Young's modulus  $E_t$  plus 2 parameters to describe the Poisson's ratio  $\nu_t$  plus 1 parameter to describe the unloading-reloading path modulus  $E_{ur}$ . The 7 parameters for  $E_t$  included the unit weight  $\gamma$ , the coefficient of earth pressure at rest  $K_0$ , the initial tangent modulus factor  $K$ , the stress influence exponent  $n$  for the tangent Young's modulus, the failure ratio  $R_r$ , the effective stress friction angle  $\phi$  and the effective stress cohesion  $C$ . The 2 additional parameters for  $\nu_t$  were the bulk modulus factor  $K_b$  and the stress influence exponent  $n_b$  for the bulk modulus. The additional parameter for  $E_{ur}$  was the unload-reload modulus factor  $K_{ur}$ .

The tangent Young's modulus  $E_t$  is defined as the instantaneous tangential slope of the triaxial stress strain curve

$$E_t = \frac{\partial(\sigma_1 - \sigma_3)}{\partial \epsilon_1} \quad (1)$$

where  $\sigma_1$ , and  $\sigma_3$  are the major and minor principal stresses in a soil element, and  $\epsilon_1$  is the major principal strain for that same soil element. The expression that gives  $E_t$  for the hyperbolic model is:

$$E_t = \left[ 1 - \frac{R_r(1 - \sin\phi)(\sigma_1 - \sigma_3)}{2(c \cos\phi + \sigma_3 \sin\phi)} \right]^2 K P_a \left( \frac{\sigma_3}{P_a} \right)^n \quad (2)$$

where  $\sigma_1$ , and  $\sigma_3$  have initial values of  $\gamma z$  and  $K_0 \gamma z$  ( $z$ =depth) which are updated as the loading and unloading take place in increments, and  $P_a$  is the atmospheric pressure. The unload-reload modulus  $E_{ur}$  is given by:

$$E_{ur} = K_{ur} P_a \left( \frac{\sigma_3}{P_a} \right)^n \quad (3)$$

The tangent Poisson's ratio  $\nu_t$  is defined as:

$$\nu_t = 0.5 - \frac{E_t}{6B_t} \quad (4)$$

where that tangent bulk modulus  $B_t$  is given by:

$$B_1 = K_B P_a \left( \frac{\sigma_3}{P_a} \right)^{n_B} \quad (5)$$

This hyperbolic model was coded in FORTRAN and implemented into ABAQUS as a user defined subroutine UMAT.

## 5. Simulating the Excavation Sequence

In conventional FE analyses of tieback walls, two dimensional plane strain conditions are assumed and widely accepted. While the load pattern of the anchors is repetitive along one elevation, it is not necessarily continuous. Furthermore, if the wall consists of repetitive arrangement of soldier piles and tiebacks, the wall cannot be assumed as plane strain condition. Therefore plane strain assumptions are not correct in this kind of load pattern and wall configuration.

The initial shape of the mesh was a rectangular parallelepiped (Fig. 5). The first step was to turn on the gravity stresses in that large brick which was 76m long, 16.5m high, and 2.44m wide (Fig. 6). The second step was to install the piles; this consisted of activating the beam elements and allowing them to be stressed by the steps. Therefore driving stresses were not simulated. The third step was to excavate the first lift (2.4m in the case history). This step induced initial deflections and a change in stress. The fourth step was to install the wood lagging and to install the first row of anchors. This step consisted of activating the shell elements simulating the wood lagging, of activating the beam elements simulating the tendon bonded length of the anchor, and allowing them to be stressed by the next steps. The fifth step was to stress the anchor. This was simulated by applying on

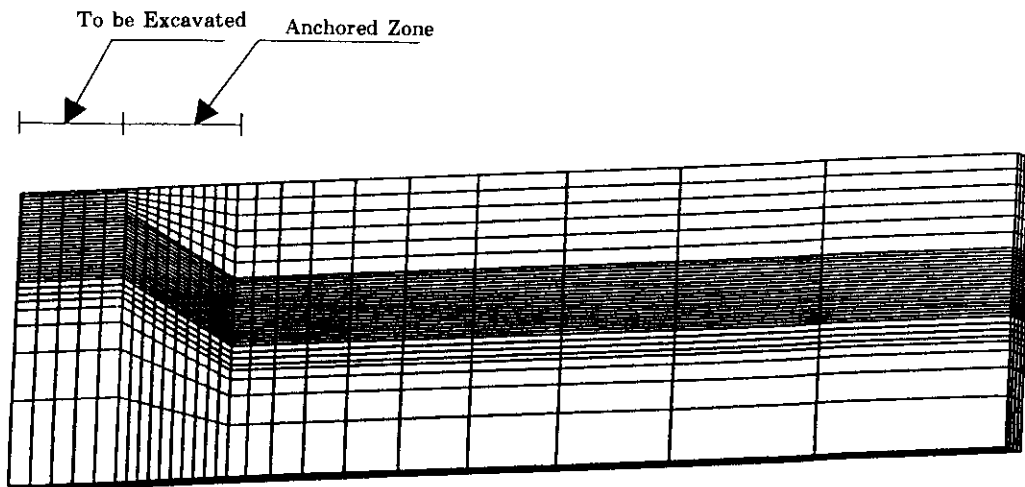
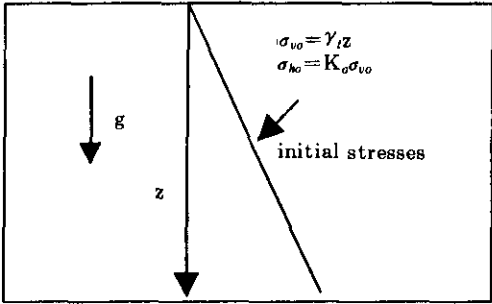
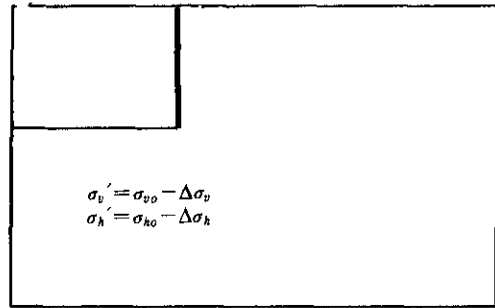


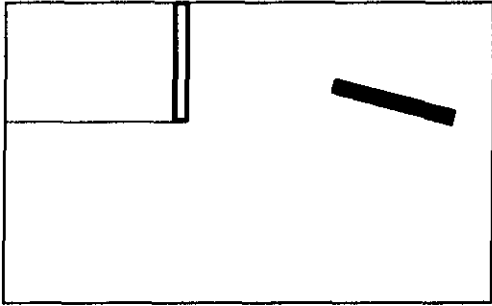
Fig.5 Finite Element Mesh



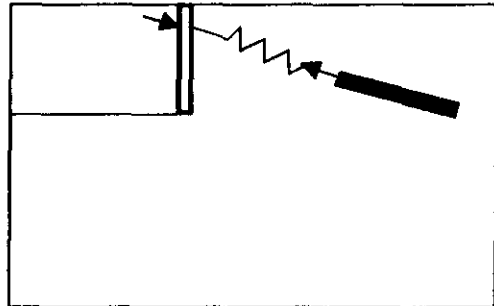
STAGE 1. Specify initial geostatic stress condition, and apply gravity load to the mesh and check equilibrium



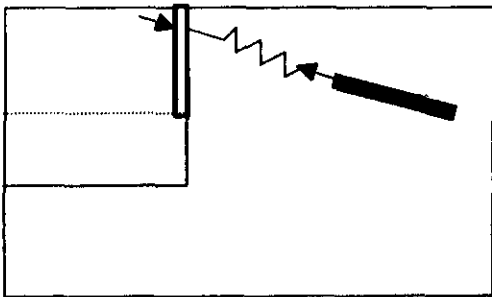
STAGE 2. Excavate to the first excavation level and install soldier pile



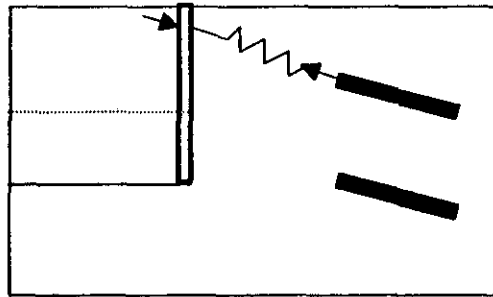
STAGE 3. Install tendon bonded zone of the first anchor row and wall facing



STAGE 4. Apply lock-off load and install tendon unbonded zone of the first anchor row



STAGE 5. Do next excavation



STAGE 6. And so on to final excavation

Fig.6 Simulation of the Excavation Sequence



the soldier pile a force  $F$  equal to and in the direction of the anchor force and applying the same force  $F$ , but in the opposite direction, at the top of the tendon bonded zone (Fig. 4). The sixth step consisted of activating the spring element simulating the unbonded tendon length. The seventh step was the excavation of the next lift. The following steps were repetitions of steps 4 to 7 to simulate additional excavation lifts and anchor stressing. The final step was an excavation step to final grade below the last rows of anchor. Each run required about 6 hours of CPU time on the Texas A&M University Super Computer (SGI Power Challenge 1000XL).

Conceptually, each excavation was simulated by applying on each element along the  $n^{\text{th}}$  excavation boundary a stress vector  $\Delta\sigma_n$  in opposite direction to the stress vector which existed on that boundary at the end of the  $(n-1)^{\text{th}}$  excavation step. The stress vector  $\Delta\sigma_n$  was found by iteration until that vector and the stress vector existing on that boundary at the end of the previous step added to zero all along the  $n^{\text{th}}$  excavation boundary. All elements above the  $n^{\text{th}}$  excavation boundary were then deactivated.

The solution of an excavation problem in nonlinear finite element analyses can be obtained by the following procedures:

1. At each excavation step the unbalanced forces due to the excavation of the soil layers are:

$$K^n \Delta U^n = P^n - I^{n-1} = R^n \quad (6)$$

where  $K^n$  is the tangent global stiffness matrix for the active elements at the current increment or iteration,  $\Delta U$  are the increments of nodal point displacements,  $P^n$  are the external loads for the current active elements,  $I^{n-1}$  are the internal forces for active elements resulting from the previous excavation step,  $R^n$  is the residual force vector. Effects of external loads such as gravity loads may be reflected in  $P^{n-1}$ . Effects of internal stresses are reflected in  $I^{n-1}$ .

2. Solve for the residual force vector  $R$  assuming elastic behavior. For each excavation step the force vector  $R$  is applied in several increments. Then, equilibrium is found by iterating to reach a certain tolerance. For a system which is exactly in equilibrium  $R^n=0$ .
3. Compute the internal force vector  $I^{n-1}$  for elements in the  $n^{\text{th}}$  excavation stage by considering stresses existing after  $(n-1)^{\text{th}}$  excavation.
4. Compute the residual forces.
5. If convergence does not occur, apply the residual forces instead of  $R$  and repeat steps 2-4.
6. If convergence occurs, go to step 1: solve for the next step of excavation.

## 6. Texas A&M University Instrumented Tieback Wall

The Federal Highway Administration and Schnabel Foundation sponsored the construc-

tion of a full scale instrumented tieback wall in 1991 at the National Geotechnical Experimentation Site(NGES) on the Riverside Campus of Texas A&M University(Fig. 7). This wall is 60m long and 7.5m high. It was built by driving H piles in a line on 2.44m center for one part of the wall. One half of the wall had only one row of anchors while the other half had two rows of anchors. The two row anchors wall was used to calibrate the FEM model. The steel H piles were HP 6×25 sections, 9.15m long embedded 1.65m below the bot-

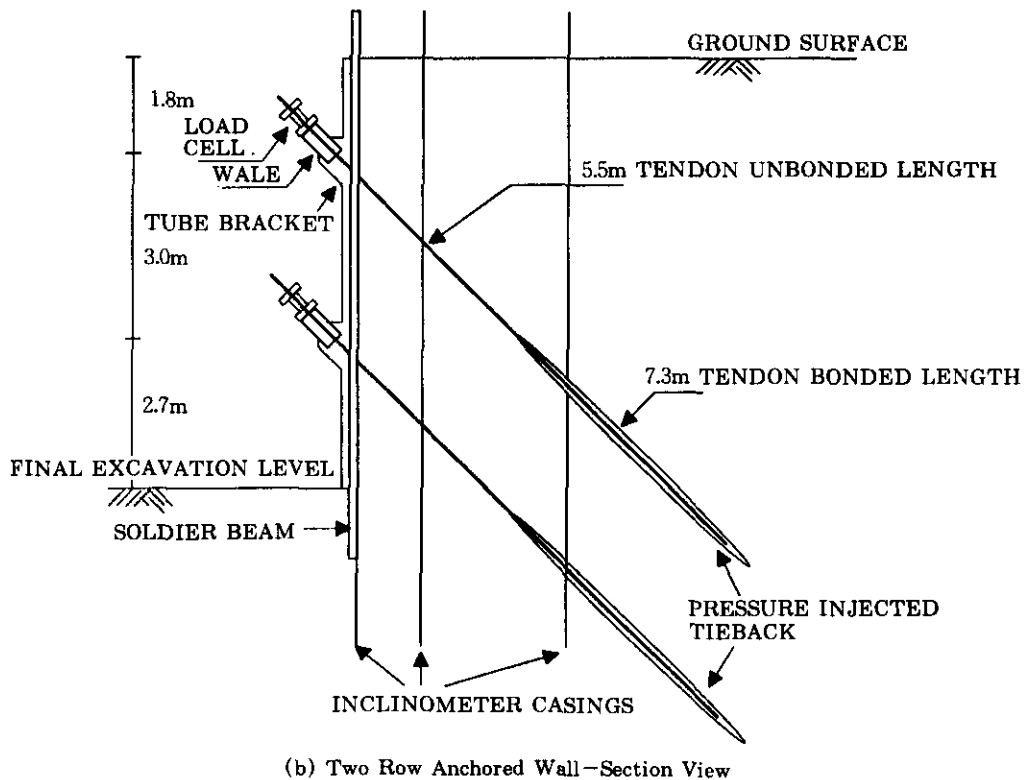
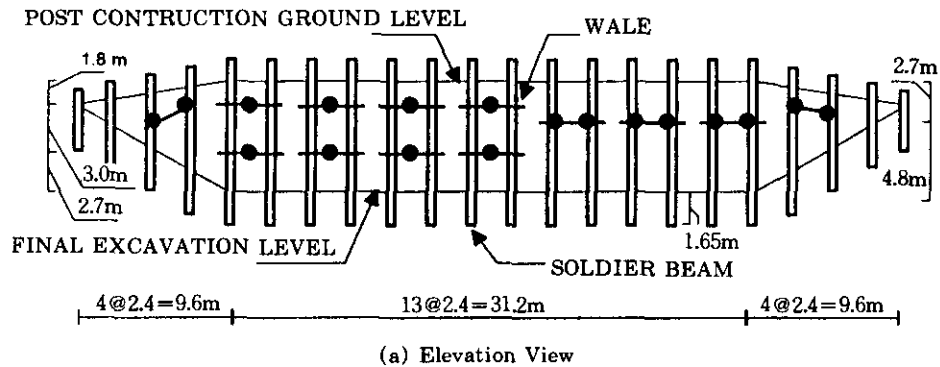


Fig.7 The Texas A & M University Tieback Wall

tom of the excavation. The lagging boards were 2.4m long, 0.3m high and 75mm thick. The high pressure grouted anchors were inclined  $30^\circ$  with the horizontal and located at 1.8m and 4.8m below the top of the wall; they were 89mm in diameter, 12.35m long with a 7.3m tendon bonded length.

The soil consists of a 13m thick layer of medium dense fine silty sand deposited in a river environment about 50 thousand years ago and underlain by a 40 million year old hard shale. The engineering properties and the geology of this sand deposit have been determined in detail as part of the NGES program (Briaud, 1992; Marcontel and Briaud, 1994; Tao and Briaud, 1995; Simon and Briaud, 1996; Jennings et al., 1996; McClelland Engineers, 1996). The sand has the following average properties: total unit weight  $18.5 \text{ kN/m}^3$ , SPT blow count increasing from 10 blows/0.3m at the surface to 27 blows/0.3m at the bottom of the soldier piles, borehole shear friction angle  $32^\circ$  with no cohesion, CPT point resistance 7 MPa, PMT modulus 8 MPa, PMT limit pressure 0.5 MPa. The water level is 9.5m below the top of the wall.

The wall was instrumented with vibrating wire strain gauges on the soldier piles to obtain bending moment profiles, with inclinometer casings to obtain horizontal deflection profiles, and with load cells at the anchor heads to monitor the anchor forces.

## 7. Calibration of Model Against Texas A&M University Two Row Anchor Tieback Wall

The TAMU two row anchor tieback wall was used to calibrate the FEM model. The H piles were replaced with pipe piles of equivalent stiffness (AE and EI) because the H piles created some numerical instabilities. For the anchors, the grout annulus with a modulus equal to 0.4 times the intact modulus of grout was included with the steel tendon to compute the stiffness AE and EI of the tendon bonded length. The 10 parameter hyperbolic model was used for the soil.

The calibration process consisted of finding the set of those 10 parameters which led to the best match between the measured and calculated deflection  $u$ , bending moment  $M$  and axial load  $Q$  profiles of the soldier piles. It was found that the most influential parameters were  $K$  and  $K_0$  for the deflections,  $E_{wood}$  and  $K_0$  for the bending moment,  $\gamma_1$  for the axial load including the downdrag load. All other parameters had a relatively small impact on the calculated values.

The comparison between measured and calculated  $u$ ,  $M$  and  $Q$  profiles were shown in Fig. 8. The final parameters are presented in Table 1.

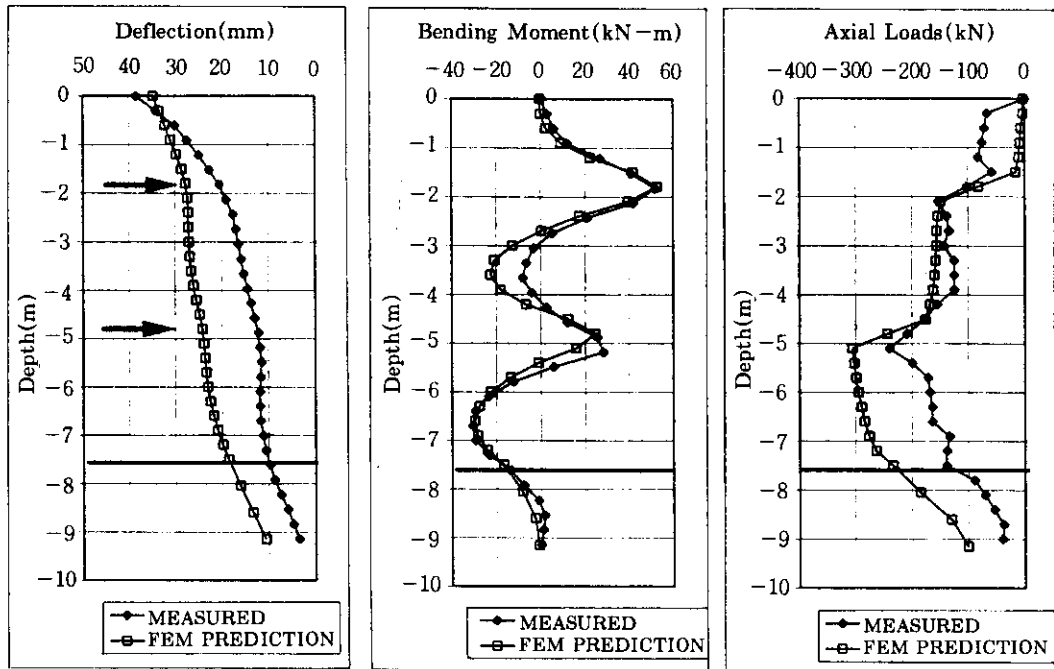


Fig.8 Measured and Calculated Displacements( $u$ ), Bending Moments( $M$ ), and Axial Loads( $Q$ )

Table 1. Parameters Used for the FEM Simulation

Soil Data	Initial tangent modulus factor, $K$	300
	Initial tangent modulus exponent, $n$	0.85
	Strength ratio, $R_f$	0.93
	Friction angle, $\phi$	$32^\circ$
	Cohesion, $c$	0
	Unloading-reloading modulus number, $K_{ur}$	1200
	Bulk modulus number, $K_B$	272
	Bulk modulus exponent, $n_B$	0.5
	Unit weight, $\gamma_s$	$18.5 \text{ kN/m}^3$
	At rest earth pressure coefficient, $K_0$	0.65
Anchor Data	Tendon unbonded length	5.5m
	Tendon bonded length	7.3m
	Lock-off load-row1	182.35kN
	Lock-off load-row2	160.0kN
	Tendon stiffness-row1	$19846 \text{ kN/m}$
	Tendon stiffness-row2	$19479 \text{ kN/m}$
	Angle of Inclination, $\beta$	$30^\circ$

Wall Facing Data	Wall height	7.5m
	Thickness of wall facing	0.1m
	Elastic modulus of wood board	$1.365 \times 10^6 \text{ kN/m}^2$
Soldier Pile Data	Length of soldier pile	9.15m
	Embedment	1.65m
	Diameter of pipe pile	0.25m
	Thickness of pipe pile	0.00896m
	Horizontal spacing of piles	2.44m
	Elastic modulus of steel pipe pile	$2.1 \times 10^8 \text{ kN/m}^2$
	Flexural stiffness, EI	11620kN-m <sup>2</sup>
	Axial stiffness, AE	$1.47 \times 10^6 \text{ kN}$

## 8. Parametric Analysis

A number of factors were varied from the initial values of the case history in order to evaluate their influence on the design (Table 2.). These factors were the location of the anchor, the length of the tendon unbonded zone, the magnitude of the anchor forces, the embedment of the soldier piles, the stiffness AE and EI of the wood lagging, and the stiffness AE and EI of the soldier piles.

The location of the first anchor (Y) was varied from 0.6m to 1.8m below the top of the wall. The second anchor was kept 3m below the first anchor. The results show (Fig. 9) that a position of 1.2 to 1.5m leads to lower deflections and lower bending moments with a 25% reduction in  $u$  and  $M$  compared to the 1.8m anchor position. The results also show that the position of the first anchor has very little influence on the axial load distribution including the downdrag load.

The length of the tendon unbonded zone  $L_u$  was about 5m for the case history. This length  $L_u$  was varied from 1.375m to 16.2m while keeping the tendon bonded length constant and equal to 7.3m. The results show (Fig. 10) that  $L_u$  only has a small influence on the bending moment and the axial load in the soldier piles as long as the beginning of the tendon bonded zone is outside the failure wedge. The unbonded length  $L_u$  has a significant influence on the deflection at the top of the wall  $u_{top}$ ; when  $L_u$  was 3 times longer than in the case history, the deflection at the top of the wall  $u_{top}$  was equal to 0.57 times the value of  $u_{top}$  for the case history. It was found that  $L_u$  had no influence on the deflection at the bottom of the wall which remained equal to 10mm. It was also found that increasing  $L_u$  for the first anchor alone was much more effective to reduce deflection than increasing  $L_u$  for the second anchor.

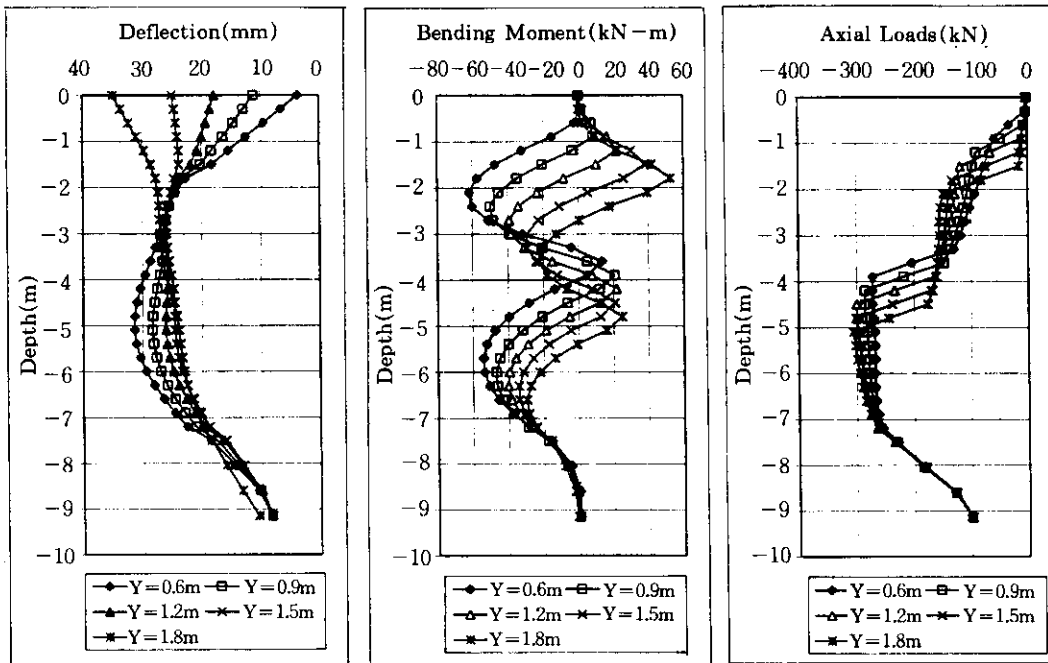


Fig.9 Influence of First Anchor Location (Y=Depth)

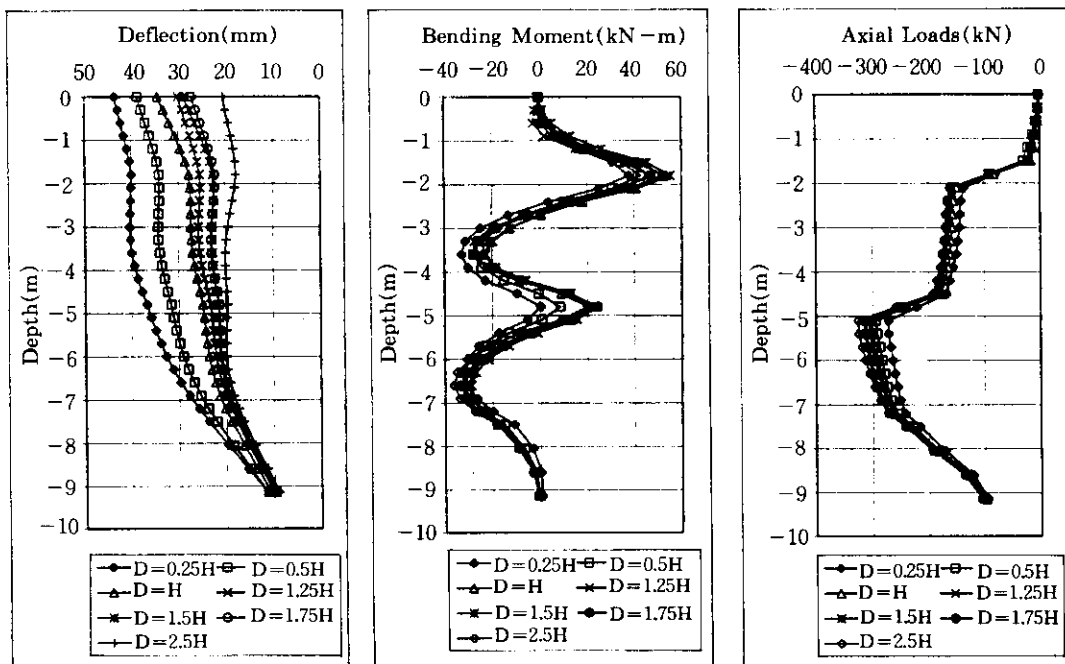


Fig.10 Influence of Tendon Unbonded Length

The magnitude of the anchor force was varied. The sum of the horizontal components of the anchor forces divided by the frontal area of the wall is the average pressure  $p$  corresponding to a constant pressure diagram against the wall. The ratio of  $p$  over  $\gamma H_t$  is the earth pressure coefficient  $K$ ;  $\gamma$  is the effective soil unit weight and  $H_t$  is the total height of the wall. The value of the  $K$  was varied in the parametric analysis from 0.02 to 1.1 by varying the anchor loads correspondingly and the deflection at the top of the wall  $u_{top}$  was calculated by the FEM. Case histories were also collected to obtain measured values of  $K$  and corresponding measured value of  $u_{top}$ . The Boston case history was obtained from Houghton and Dietz (1990), the Bonneville case history was obtained from Munger et al. (1990), the Lima case history was obtained from Lockwood (1988), and the Texas A&M University case history was obtained from Chung and Briaud (1993). The relationship between  $K$  and  $(u_{top}/H_t)$  is presented in Fig. 11, while the relationship between  $K$  and  $((u_{mean}/H_t))$  is in Fig. 12. These figures show that for the common values of  $K$  equal to  $0.65K_a$  used in design, the ratio  $(u_{top}/H_t)$  varies from  $1/500$  to  $1/225$  depending on a number of factors including  $L_e$ . For the same value of  $K$ , the ratio  $(u_{mean}/H_t)$  varies from  $1/1000$  to  $1/300$ . The figures also show that for  $K$  values of about 0.4 the deflections are close to zero and that  $K$  values higher than 0.4 the wall moves inward.

The embedment of the soldier piles was varied from 0m to 10m. The results show that  $u_{top}$  decreases with increasing embedment (Fig. 13), that the bending moment profile does not

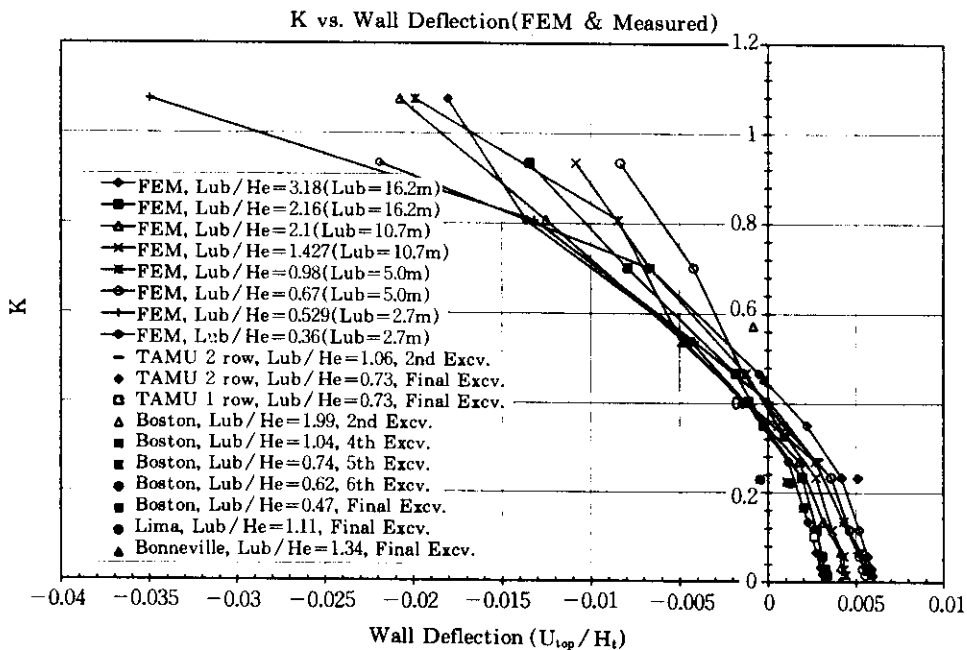


Fig.11 Influence of Anchor Force on the Deflection at the Top of the Wall

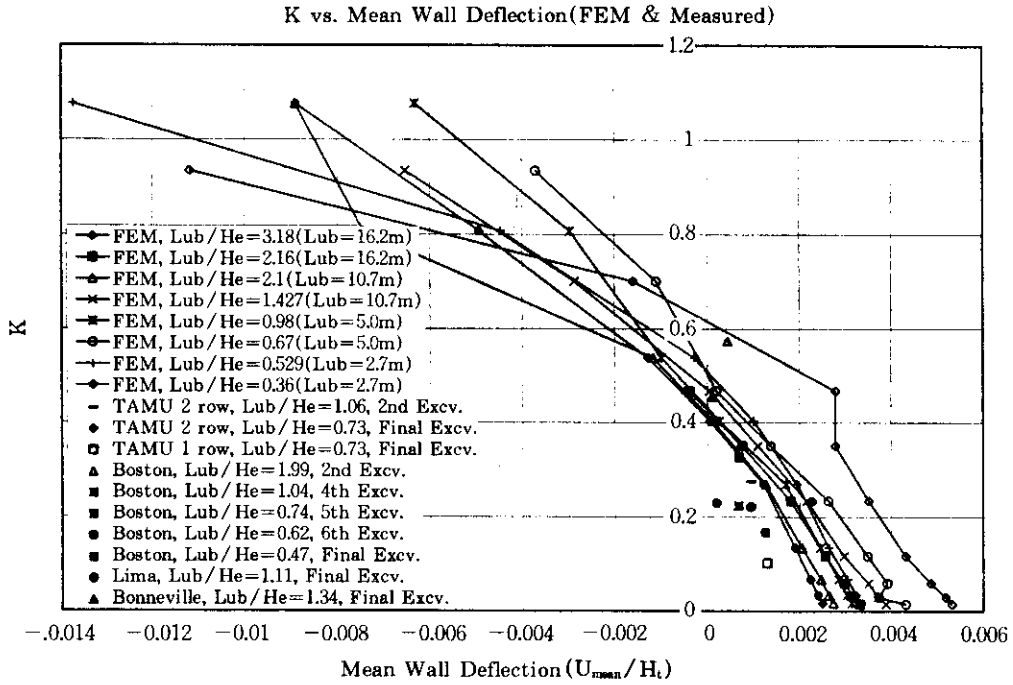


Fig.12 Influence of Anchor Force on the Mean Wall Deflection

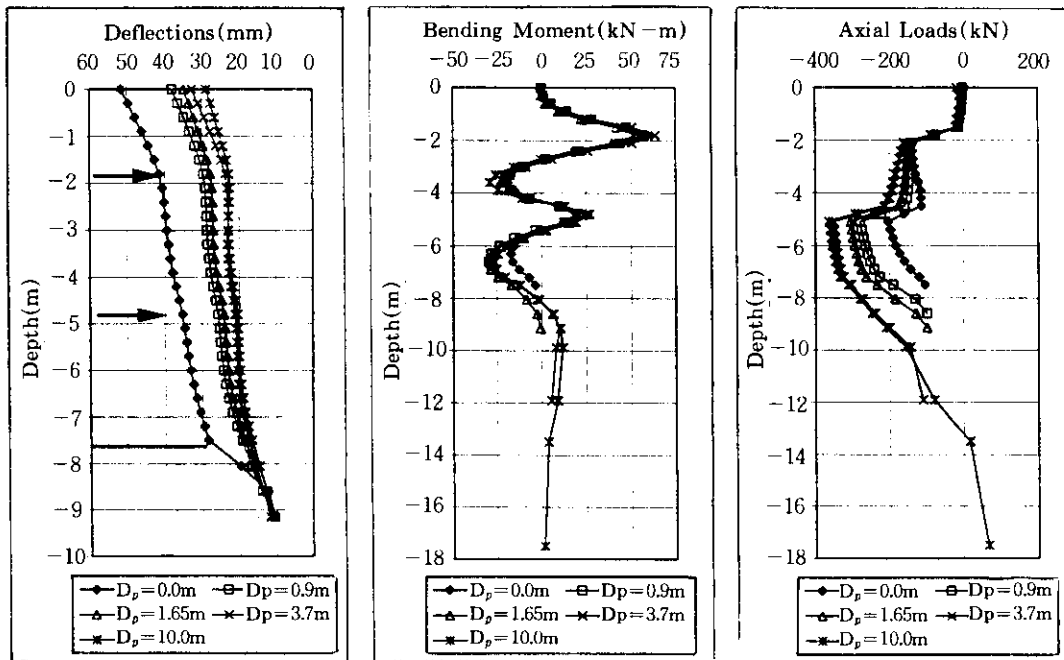


Fig.13 Influence of Soldier Pile Embedment



Table 2. Parameters Used for the Parametric Study of Tieback Wall

No.	Unbonded Length $L_{UB}$	Anchor Load Level P	First Anchor Depth Y	Embedment $D_P$
1	1.375m	P/8	0.6m	0.0m
2	2.7m	P/4	0.9m	0.9m
3	5.0m	P/2	1.2m	1.65m
4	7.3m	P	1.5m	3.7m
5	8.93m	2P	1.8m	10.0m
6	10.7m	4P		
7	16.2m	8P		

\*  $L_{UB}$  is represented as the distance (D) from top of wall to inclined anchorage location at the ground surface, times wall height ( $H=7.5m$ ) as shown in Fig. 9.

change significantly, but that the downdrag load increases significantly with increasing embedment.

The modulus of the wood lagging  $E_{wood}$  was varied. With the  $E_{wood}$  value equal to the wood modulus, the wooden boards bow between the soldier piles and the center of the wooden boards deflects more than the piles. As  $E_{wood}$  increases the boards become more rigid and the boards and soldier piles tends toward a common deflection: as a result the piles deflection increases. The bending moment also increases but the axial load is relatively unaffected. Varying the stiffness of the soldier piles has only a small influence on the deflections, bending moments and axial loads.

## 9. Conclusions and Design Implications

The following recommendations are based on the data from four case histories, on a detailed three dimensional nonlinear Finite Element Method simulation of one of these case histories and on an extensive FEM parametric analysis. The application of these recommendations is limited by the range of parameters studied.

The best position for the first anchor appears to be between 1.2 and 1.5m below the top of the wall. In current practice the first anchor tends to be placed deeper than that; significant deflections can accumulate during this step and it is very difficult to eliminate them by further construction. By comparison in soil nailing, the first nail is placed at a much shallow depth. A vertical spacing of 3m between anchor rows below the first anchor appears to work well.

The length of the unbonded length proposed by Cheney (1988) seems to work well (Fig. 14.). Longer unbonded zones particularly for the first anchor leads somewhat smaller deflections.

The magnitude of the anchor loads is the most important factor influencing all variables. It has a direct influence on deflections and bending moments. In the case of mechanically

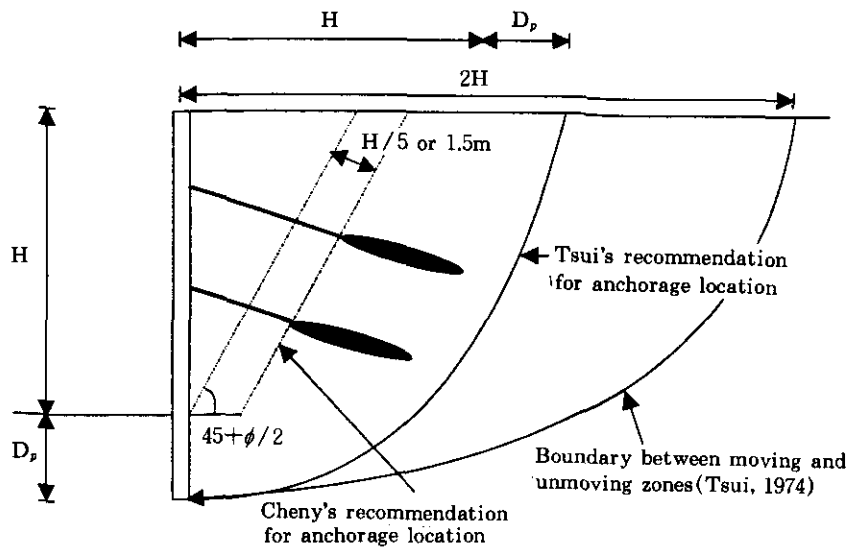


Fig.14 Recommended Anchorage Locations by Cheney(1988) and by Tsui(1974):  
 $D_p$ =Embedment of Soldier Pile

stabilized earth walls and soil nailed walls, deflections are largely uncontrolled. In the case of tieback walls, the engineer can now use the the proposed  $K$  vs.  $(u_{top}/H_t)$  relationship to select anchor loads which will approximately generate a chosen deflection. Zero deflection can be reached for a constant pressure diagram with a pressure intensity equal to  $0.4\gamma H_t$ . This pressure is approximately 2 times larger than Terzaghi and Peck intensity equal to  $0.65K, \gamma H_t$ .

Providing no embedment for the soldier piles is not recommended even if bottom heave and slope stability do not raise problems. No embedment leads to larger deflection. An embedment of 1.5m decreased the top deflection significantly in this study.

### Acknowledgements

This project was sponsored by the Texas Department of Transportation (Mr. Mark McClelland), the Texas A&M University Super Computer Center (Dr. Spiros Vellas), and the Federal Highway Administration (Mr. Al DiMillio).

### References

1. ABAQUS User's and Theory Manuals. 1992, Version 5.2, Hibbit, Karlson, and Sorensen Inc., Pawtucket, R.I., U.S.A.
2. Briaud, J.L. (1993). "National Geotechnical Experimentation Site at Texas A&M University:

- Data Collected Until 1992." Report No. NGES-TAMU-001, Department of Civil Engineering, Texas A&M University, College Station.
3. Chung, M., and Briaud, J. L. (1993). "Behavior of a Full Scale Tieback Wall in Sand." Report to Schnabel Foundation and The Federal Highway Administration, Department of Civil Engineering, Texas A&M University, College Station.
  4. Clough, W. G. (1984). "User's Manual for Program SOILSTRUCT." Department of Civil Engineering, Virginia Polytechnic Institute, Blacksburg, Virginia, U.S.A.
  5. Duncan, J. M., Byrne, P. M., Wong, K. S., and Marby, P. (1980). "Strength, Stress-strain and Bulk Modulus Parameters for Finite Element Analyses of Stresses and Movements in Soil Mass." Report No. UCB/GT/80-01, University of California, Berkeley.
  6. Dunlop, P., and Duncan, J. M. (1970). "Development of Failure Around Excavated Slopes." J. of Soil Mech. and Found. Div., ASCE, Vol. 96, No.2, 471-493.
  7. Fugro-McClelland. (1996). "National Geotechnical Experimentation Sites at Texas A&M University: Clay and Sand Laboratory Test Data." Report No. NGES-TAMU-007, Department of Civil Engineering, Texas A&M University, College Station.
  8. Haliburton, T. A. (1968). "Numerical Analysis of Flexible Retaining Structures." Proceedings, ASCE, Vol. 94, SM3, 1233-1251, ASCE, New York, U.S.A.
  9. Houghton, R. C., and Dietz, D. L. (1990). "Design and Performance of a Deep Excavation Supports in Boston, Massachusetts." Proc. ASCE Spec. Conf. On Design and Performance of Earth Retaining Structures, ASCE, New York, U.S.A.
  10. Jennings, S. P., Mathewson, C. C., Yancey, T. E., and Briaud, J. L. (1996). "National Geotechnical Experimentation Sites at Texas A&M University: Clay and Sand Geology." Report No. NGES-TAMU-005, Department of Civil Engineering, Texas A&M University, College Station.
  11. Kim, N. K., and Briaud, J. L. (1994). "A Beam Column Method for Tieback Walls." Report to Schnabel Foundation and the Federal Highway Administration, Department of Civil Engineering, Texas A&M University, College Station, Texas, U.S.A.
  12. Lim, Y.-J. (1996). "Three-Dimensional Nonlinear Finite Element Analysis of Tieback walls and of Soil Nailed Walls Under Piled Bridge Abutments." Ph.D. Dissertation, Texas A&M University, College Station, Texas, U.S.A.
  13. Lim, Y.-J., and Briaud, J. L. (1996A). "Three Dimensional Nonlinear Finite Element Analysis of Soil Nailed Wall Under Piled Bridge Abutments and Design Applications" Report to the Federal Highway Administration, Department of Civil Engineering, Texas A&M University, College Station, Texas, U.S.A.
  14. Lim, Y.-J., and Briaud, J. L. (1996B). "Three-Dimensional Nonlinear Finite Element Analysis of Tieback walls and of Soil Nailed Walls Under Piled Bridge Abutments." Report to the Federal Highway Administration and the Texas Department of Transportation, Department of Civil Engineering, Texas A&M University, College Station, Texas, U.S.A.
  15. Lockwood, M. E. (1988). "Retention System Monitoring Demonstration Project No.68." Report for the Ohio Department of Transportation, Cincinnati, Ohio, U.S.A.
  16. Marcontell, M., and Briaud, J. L. (1994). "National Geotechnical Experimentation Sites at Texas A&M University: Clay and Sand. Data Collected Until 1994." Report No. NGES-TAMU-003, Department of Civil Engineering, Texas A&M University, College Station.
  17. Matlock, H., Bogard, D., and Lam, I. (1981). "BMCOL76: A Computer Program for the Analysis of Beam-Columns Under Static Axial and Lateral Loading." Program developed at the University of Texas at Austin, under grant from Fugro Inc., and documented at Ertec Inc., Long Beach, California, U.S.A.

18. Munger, D. F., Jones, P. T., and Johnson, J. (1990). "Temporary Tieback Wall, Bonneville Navigation Lock." Proc. ASCE Spec. Conf. n Design and Performance of Earth Retaining Structures, ASCE, New York, U.S.A., 778-794
19. Simon, P. A., and Briaud, J. L. (1996). "The National Geotechnical Experimentation Sites at Texas A&M University: Clay and Sand, Soil Data in Electric Form 1995-1996." Report No. NGES-TAMU-006, Department of Civil Engineering, Texas A&M University, College Station.
20. Palazzolo, A. B. (1992). "Finite and boundary elements for structural , field, and lubrication applications.", Lecture Note Vol. 1, Texas A&M University.
21. Pfister, P. G., Evers, M., Guillaud, M., and Davidson, R. (1982). "Permanent Ground Anchors, Soletanche Design Criteria.", FHWA/RD-81/150, U.S. Dept. of Teansportation
22. PATRAN, Patran Plus User's Manual, PDA Engineering, U.S.A.
23. Terzaghi, K., and Peck, R. B. (1967). "Soil Mechanics in Engineering Practice." John Wiley and Sons, 2nd ed., New York, U.S.A.
24. Tsui, Y. (1974). "A Fundamental Study of Tied-back Wall Behavior." Ph.D. Dissertation, School of Engineering, Duke University, Durham, North Carolina.
25. Xanthakos, P. P. (1991). "Ground Anchors and Anchored Structures.", John Wiley & Sons, Inc., New York.2

(received Apr. 9, 1997)